

# Hysteresity effects in 3 mol% yttria-doped zirconia ( $t'$ -phase)

K. M. PRETTYMAN, J.-F. JUE, A. V. VIRKAR

*Department of Materials Science and Engineering, University of Utah, 304 EMRO, Salt Lake City, UT 84112, USA*

C. R. HUBBARD, O. B. CAVIN, M. K. FERBER

*Oak Ridge National Laboratory, Oak Ridge, TN 37831, USA*

Single-crystal and polycrystal samples of 3 mol%  $Y_2O_3$ -doped zirconia ( $t'$ -phase) were subjected to uniaxial compression tests at 1000 °C in order to separate the effects of phase transformation (tetragonal-to-monoclinic) from ferroelastic domain switching. Plastic deformation was observed after an elastic regime, with attributes characteristic of domain switching. X-ray diffraction traces at room and high temperatures before and after the compression test verified that there was, indeed, a variant reorientation within each sample. Deformation bands were observed on single crystals, and Raman spectroscopy revealed that no monoclinic phase was present. These results verify the existence of ferroelastic domain switching phenomenon in this material.

## 1. Introduction

The concept of ferroelastic behaviour being involved in phase transitions has been well defined and its study has been continuing for over 20 years [1]. It was proposed as a potential toughening mechanism in zirconia in 1986 [2]. From transmission electron microscopy (TEM) and transmission optical microscopy (TOM) techniques it is known that ferroelastic domains exist in 3 mol% yttria-doped zirconia in the  $t'$ -phase, with typical dimensions of  $0.05 \mu\text{m} \times 1.0 \mu\text{m}$  [3-7]. This previous work had been done at room temperature. Fig. 1 illustrates the "herringbone" domain structure typical in these materials.

Heretofore it had been assumed by many that the  $t'$ -phase was a "non-transformable phase", since no monoclinic phase had been observed when the sample was stressed [8]. It has been shown, however, that this is not the case, but that transformation is possible and is a function of the domain size [5, 9, 10]. The purpose of this study was to demonstrate clearly the ferroelastic domain switching phenomenon in these materials by eliminating the possibility of both the reversible and irreversible tetragonal-to-monoclinic phase transformation. This was done by eliminating the driving force for this transformation by conducting uniaxial compression tests at temperatures well above the equilibrium transition temperature between the tetragonal and monoclinic phases. For 3 mol%  $Y_2O_3$ -doped tetragonal zirconia polycrystal (TZP) this phase transition occurs at 750 °C or below, based on the available diagram [11-15]. Ferroelastic domain switching is easier at high temperatures since the coercive stress ( $\sigma_{\text{coer}}$ ) is an inverse function of temperature [16]. It is

important, however, not to exceed the Curie temperature ( $T_c$ ) of the material, since at that temperature the material no longer exists in a ferroelastic phase, but instead becomes paraelastic. In 3 mol%  $Y_2O_3$ -doped TZP this occurs when the tetragonal ferroic phase transforms into the cubic prototype phase at around 2000 °C [17, 18]. It is also necessary to choose a temperature low enough to prevent, or at least minimize, softening and plastic deformation of all test set-up materials. A temperature of 1000 °C was used in this study, since it met the above criteria.

## 2. Experimental procedure

Single-crystal and polycrystal samples were prepared in the  $t'$ -phase. The tetragonal single crystal was purchased commercially (Ceres Corporation, Waltham, MA, USA) and had been prepared using a skull melt technique. The sample was not actually a true single crystal but a "pseudo-single crystal", having three variants in mutually orthogonal directions. The irregularly shaped samples were oriented using back-reflection Laue X-ray diffraction and cut in the shape of parallelepipeds ( $3 \text{ mm} \times 3 \text{ mm} \times 9 \text{ mm}$ ) such that the faces were perpendicular to the  $\langle 100 \rangle$  directions, based on pseudocubic symmetry, as depicted in Fig. 2. They were then heated in air at 2100 °C for 15 min in a gas-fired furnace, quenched to 1200 °C and furnace-cooled to room temperature.

The polycrystalline samples were prepared using a premixed commercial powder (TZ-3Y from Tosoh USA Inc., Atlanta, GA, USA). The powder was die pressed at 28 MPa, isostatically pressed at 207 MPa

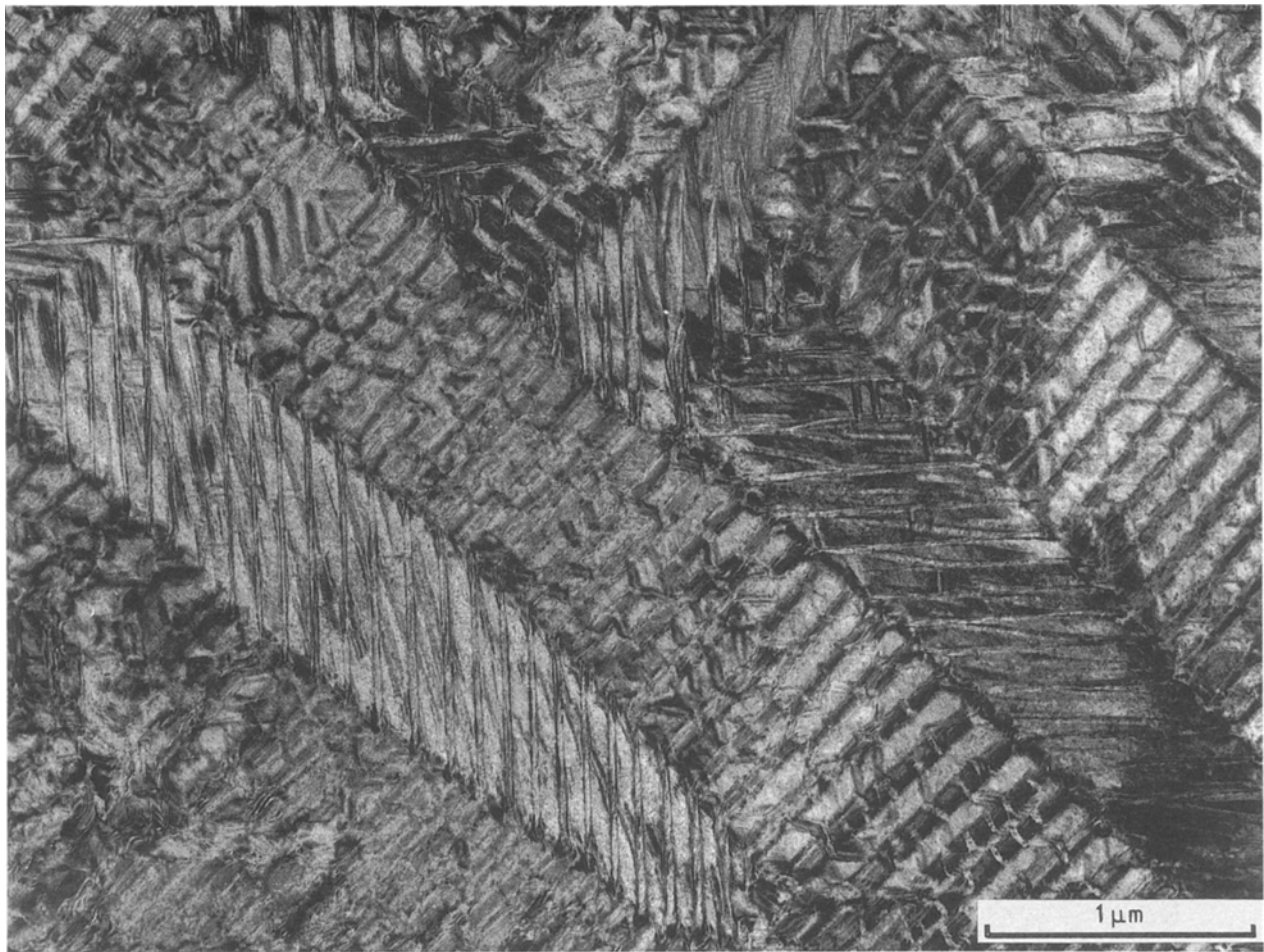


Figure 1 TEM micrograph of 3 mol %  $Y_2O_3$ -doped zirconia ( $t'$ -phase) showing existing domain structure.

and sintered in air at 1450 °C for 2 h. The sintered samples were then heated to 2100 °C for 15 min in a gas-fired furnace, quenched to 1200 °C, furnace-cooled to room temperature, and cut to size (3 mm × 3 mm × 9 mm).

A rocking-curve X-ray analysis was done on representative samples to ensure that crystallite size and preferred orientation due to processing would not significantly affect the quantitative X-ray diffraction (XRD) results. This was deemed particularly important for the polycrystalline samples after the high-temperature (2100 °C) heat treatment due to their large average grain size (> 100 μm). A rocking-curve XRD analysis is performed by making multiple XRD traces on a flat sample surface oriented at various angles to the incoming X-ray beam. This involves “rocking” the sample between  $\pm 15^\circ$  in both the  $x$ - and  $y$ -directions in order to observe whether there is a significant shift in the  $2\theta$  peak positions. Multiple X-ray diffraction traces (Scintag Pad X XRD, FRG) were obtained from various faces of all samples at room temperature and at 1000 °C before and after high-temperature testing. They were stressed in uniaxial compression at a rate of 0.01 mm min<sup>-1</sup> between two silicon carbide push-rods at 1000 °C on a universal testing machine (Instron model 6027, Boston, MA, USA). Load versus displacement was monitored during the loading–unloading cycle and a stress–strain plot was later constructed. A silicon carbide

“core sample” (6.35 mm in diameter and 12.7 mm long) was first run under the same conditions in order to determine the compliance of the loading assembly. All samples were aligned preloaded to 35 N at room temperature, and heated to 1000 °C under constant load conditions before any data were recorded.

Additional single crystals were prepared having the same  $\langle 100 \rangle$  orientation. The lateral faces were polished to a 1 μm finish and stressed in compression to 2.2 GPa at room temperature. Each face was studied before and after compression using Nomarski interference microscopy (model BH2, Olympus Optical Co., Ltd, Tokyo, Japan), XRD (model XRD-8000, Diano Corporation, Woburn, MA, USA) and laser-induced Raman spectroscopy. A triple spectrometer (model 1877C-AG, 0.6 m, triple spectrometer, Spex Industries Inc., Edison, NJ, USA) and an argon-ion laser (model 2045, Spectra Physics, Mountain View, CA, USA), operating at 488 nm, with a beam size of 5 μm diameter, were used in the Raman study. Irradiance at the sample was  $1 \times 10^9$  W m<sup>-2</sup>. A more complete discussion of the Raman technique used will be published in a separate paper [19].

### 3. Results and discussion

#### 3.1. Single crystal

The density was measured using the Archimedeian displacement technique and was determined to be

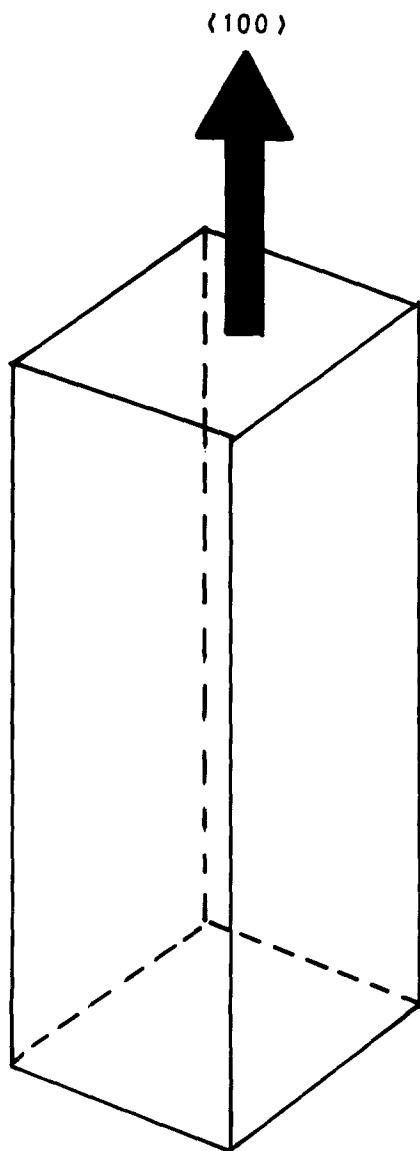


Figure 2 Orientation and dimensions of single-crystal samples.

$6.10 \text{ g cm}^{-3}$  (100% theoretical). The compressive strength was found to be  $> 2.2 \text{ GPa}$  at room temperature and  $> 400 \text{ MPa}$  at  $1000^\circ\text{C}$ . Greater stresses could not be applied for fear of damaging the test apparatus. A stress versus strain plot for this single crystal is shown in Fig. 3. The sample behaved elastically to around  $750 \text{ MPa}$ , where it began to deform plastically. Not all of the observed plastic deformation can be due to ferroelastic domain switching. Deformation due to switching is a function of the  $c/a$  ratio of the individual unit cells and of the relative percentage of cells with variants in each of the three directions. From XRD data before stressing we know that about one-third of the total number of cells exist in each of the three variant directions and that the  $c/a$  ratio is about 1.013 at room temperature and at  $1000^\circ\text{C}$ . We would therefore expect around 0.43% deformation due to ferroelastic domain switching. Here we see 1.4% plastic strain. Dislocation movement may also be occurring simultaneously at this high temperature and is discussed below.

The Young's modulus is slightly different when loading and unloading the sample. This may be due to the anisotropy in the  $[100]$  and  $[001]$  directions

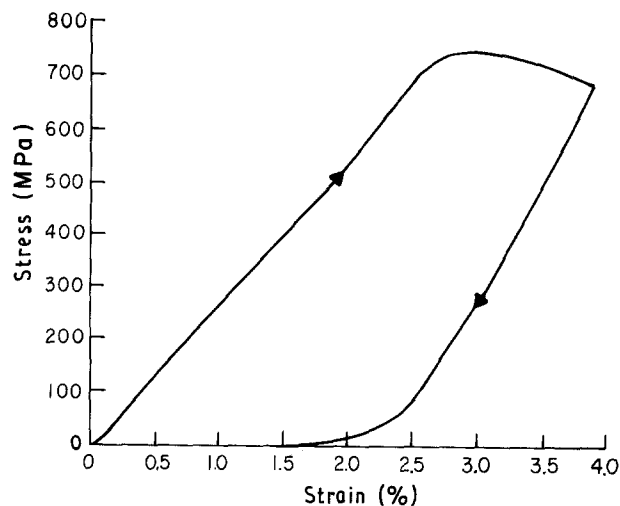


Figure 3 Stress versus strain curve for 3 mol%  $\text{Y}_2\text{O}_3$ -doped  $\text{ZrO}_2$  single crystal ( $t'$ -phase) in compression at  $1000^\circ\text{C}$  (longitudinal direction).

before and after the domain switching has occurred. After removing the effects of apparatus compliance and plasticity, the actual modulus, upon loading, at  $1000^\circ\text{C}$  is around  $127 \text{ GPa}$ , in accordance with values obtained using the free-floating beam method ( $138 \text{ GPa}$  for 3.5 mol% Y-TZP at  $1000^\circ\text{C}$ ) [20]. From the figure it is seen that some of the plastic deformation is reversible. In this case roughly half of the plastic strain produced in loading was recovered upon unloading. Part of this recovered strain can possibly be explained by data reported by Takei and Tsunekawa [21, 22]. When studying ferroelastic single crystals of neodymium niobate and lanthanum niobate, they found that the domain orientations could be switched irreversibly, or partially or completely reversibly, depending on the strain rate while loading. The strain rate was not varied in this study.

It is clear that the material exhibits quite an amount of plastic deformation, but it is not obvious that part of this deformation is due to ferroelastic domain switching, despite the occurrence of characteristics expected in switching, as previously described. However, XRD data verify this conclusion. An average overall cell orientation can be determined by observing the  $(002)/(200)$  relative peak heights and integrated intensities [14]. Table I summarizes the averages of XRD data obtained from multiple runs on the front face of the sample at room temperature. It is seen that from either the relative heights or integrated intensities, the  $(002)$  peak grows at the expense of the  $(200)$  peak, in accordance with the switching phenomenon. Fig. 4 shows some actual XRD traces from this face. Deconvolutions were done using software provided by the manufacturer of the diffractometer. XRD traces obtained from this face at  $1000^\circ\text{C}$  and on other faces at both room and high temperatures confirm these results.

Samples whose lateral faces had been polished to a  $1 \mu\text{m}$  surface finish were stressed in compression at room temperature to  $2.2 \text{ GPa}$ . The faces were observed using Nomarski interference microscopy. One such face after stress is shown in Fig. 5. A definite

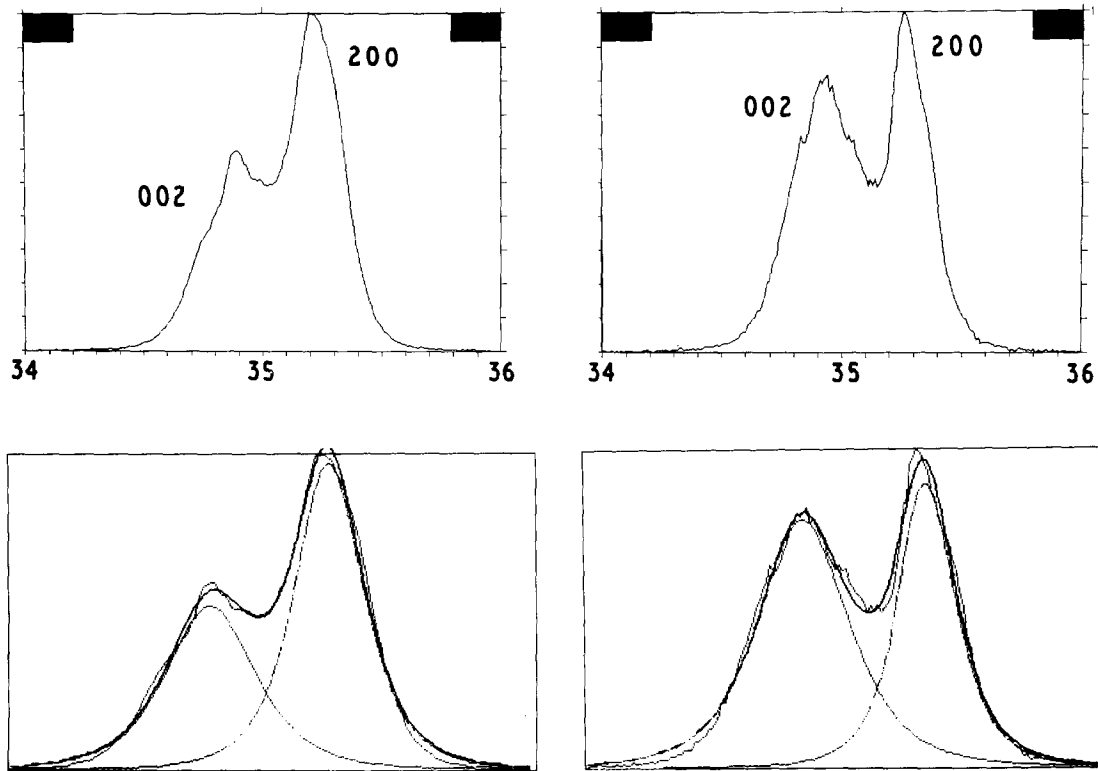


Figure 4 Room-temperature XRD traces and deconvolutions (left) before and (right) after stress in 3 mol %  $Y_2O_3$ - $ZrO_2$  ( $t'$ ) single crystal (front lateral face).

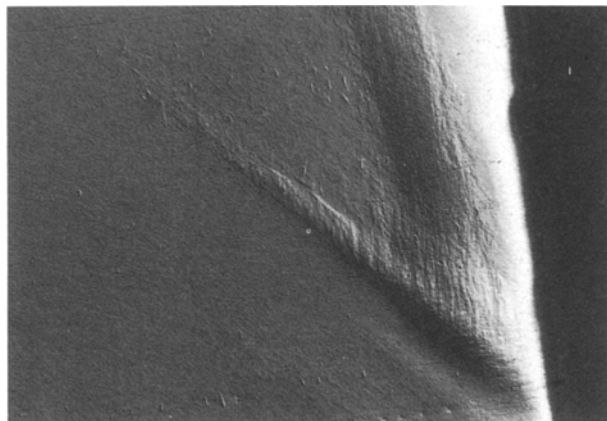


Figure 5 Nomarski interference contrast micrograph of the deformation zone produced on a lateral face during compression of a 3 mol %  $Y_2O_3$ - $ZrO_2$  ( $t'$ ) single crystal.

deformation zone has appeared due to the applied stress and can be clearly seen. XRD on the entire face showed no evidence of monoclinic phase being present. Laser-induced Raman spectroscopy was used to examine the deformation zone. The beam size was about 5  $\mu m$ . Multiple spectra were obtained in various areas within and outside the zone. One such spectrum is shown in Fig. 6. Peaks corresponding to the monoclinic phase are conspicuously absent [19, 23–25]. In fact, no monoclinic phase could be detected anywhere in the zone or on the sample surface. This finding indicates that deformation zones produced during crack propagation in zirconia, as identified by Nomarski microscopy, may not be entirely due to the

TABLE I Average values of XRD data for 3 mol %  $Y_2O_3$ - $ZrO_2$  ( $t'$ ) single crystal (front lateral face at 25°C)

	$I_{002}/I_{200}$ (peak height)	$I_{002}/I_{200}$ (integrated intensity)
Before stress	0.4	0.5
After stress	0.8	1.3

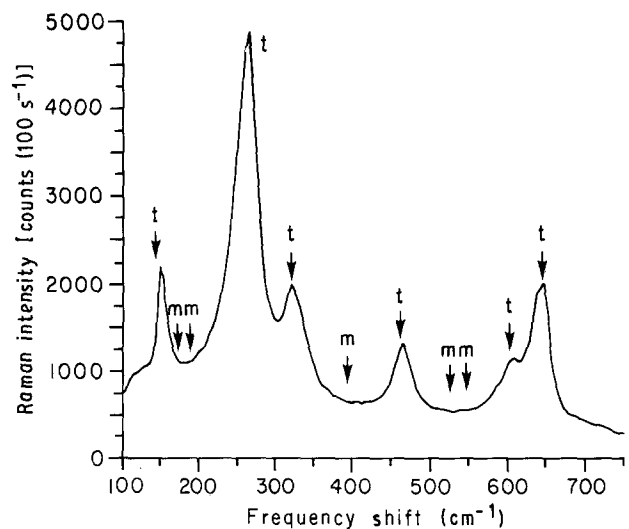


Figure 6 A typical Raman spectrum produced from inside the deformation band shown in Fig. 5. Note that no monoclinic phase is observed.

$t$ -to- $m$  phase transformation. When trying to correlate material toughness with transformation zone size (e.g. crack-shielding effects), it is important to realize that there is not necessarily a one-to-one correspondence

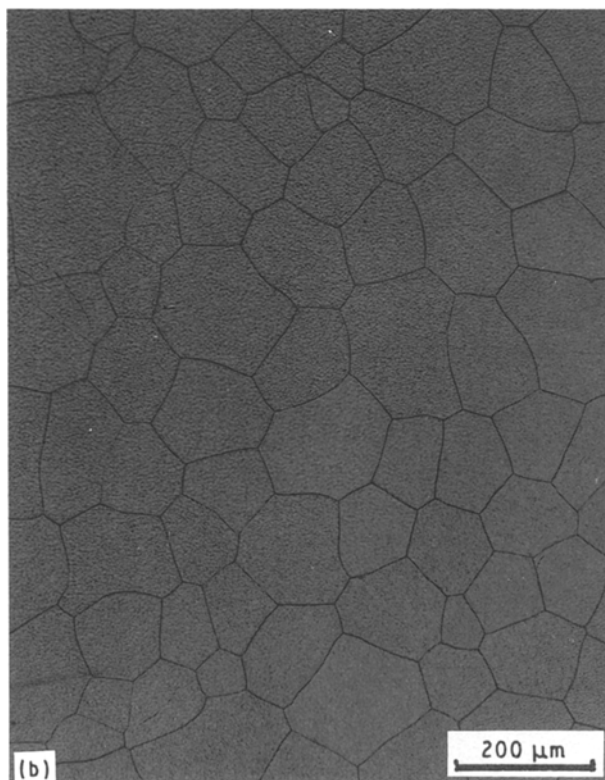
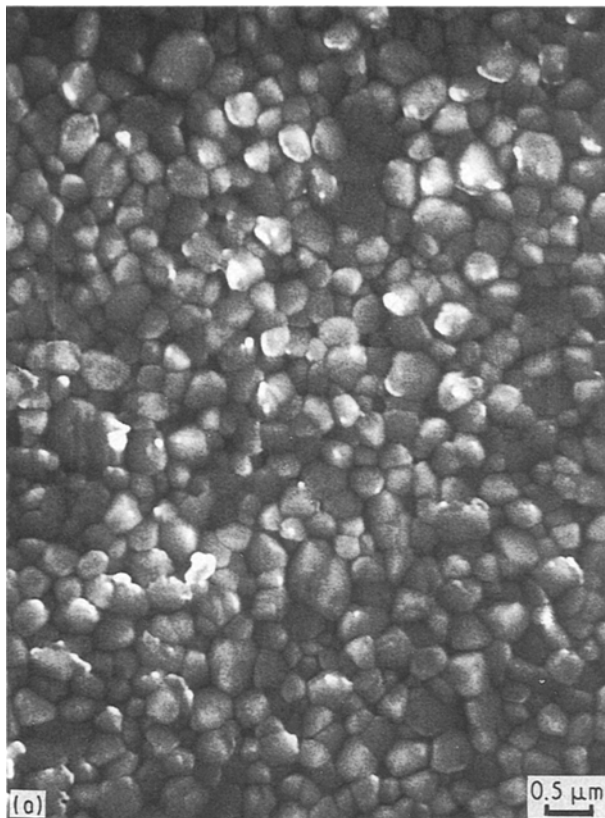


Figure 7 A scanning electron micrograph and an optical micrograph of the microstructure of 3 mol %  $Y_2O_3-ZrO_2$  ( $t'$ ) polycrystal before (grain size of around  $1 \mu m$ ) and after (grain size  $> 100 \mu m$ ) the  $2100^\circ C$  heat treatment.

between the deformation zone and the phase transformation zone.

These data also demonstrate that ferroelastic domain switching is a deformation process. Since deformation processes expend energy, some of the

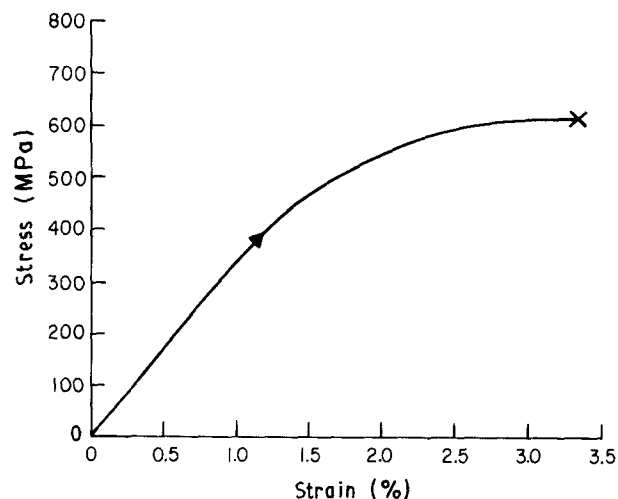


Figure 8 Stress versus strain curve to failure for 3 mol %  $Y_2O_3-ZrO_2$  ( $t'$ ) polycrystal in uniaxial compression at  $1000^\circ C$  (longitudinal direction).

mechanical energy that might normally be channelled into crack formation and extension will instead be expended in the formation and/or switching of ferroelastic domains [2]. Hence, ferroelasticity is a potential toughening mechanism.

### 3.2. Polycrystalline $t'-ZrO_2$

The density was measured to be  $6.06 \text{ g cm}^{-3}$ . The samples were translucent and no porosity was observed under an optical microscope. Due to the  $2100^\circ C$  heat treatment, the grain size in the TZP material had grown from  $0.6 \mu m$  to around  $200 \mu m$  (Fig. 7). A number of the polycrystalline  $t'-ZrO_2$  samples were first loaded in compression to failure at  $1000^\circ C$  to determine the fracture stress, as well as to ensure that the material exhibited a significant amount of plastic deformation. The compressive strength at room temperature was  $> 1200 \text{ MPa}$ . Again, the applied stress was not  $> 1200 \text{ MPa}$  for fear of damaging the fixtures in the test apparatus. A typical stress-strain curve to failure at  $1000^\circ C$  is shown in Fig. 8. The material exhibits quite an amount of plasticity beginning at  $450 \text{ MPa}$ , with the sample fracturing catastrophically at  $620 \text{ MPa}$ . After removing strain contributions from the test apparatus, about  $0.96\%$  strain was due to plastic deformation of the sample. The Young's modulus of around  $125 \text{ GPa}$  was a little lower than the value obtained for the single crystal and is consistent with data published and referred to earlier [20].

Two consecutive stress runs were made on a different sample (cut from the same "parent bar" as the sample taken to failure). The temperature was again  $1000^\circ C$ . Multiple XRD traces were obtained from various faces at room and high temperatures before and after each run. The samples were unloaded before failure occurred, but after plastic deformation had begun. Fig. 9 shows typical stress-strain plots from both runs. Again a permanent strain is observed in the material. During the first run plastic deformation began at around  $450 \text{ MPa}$ , as it did in the samples

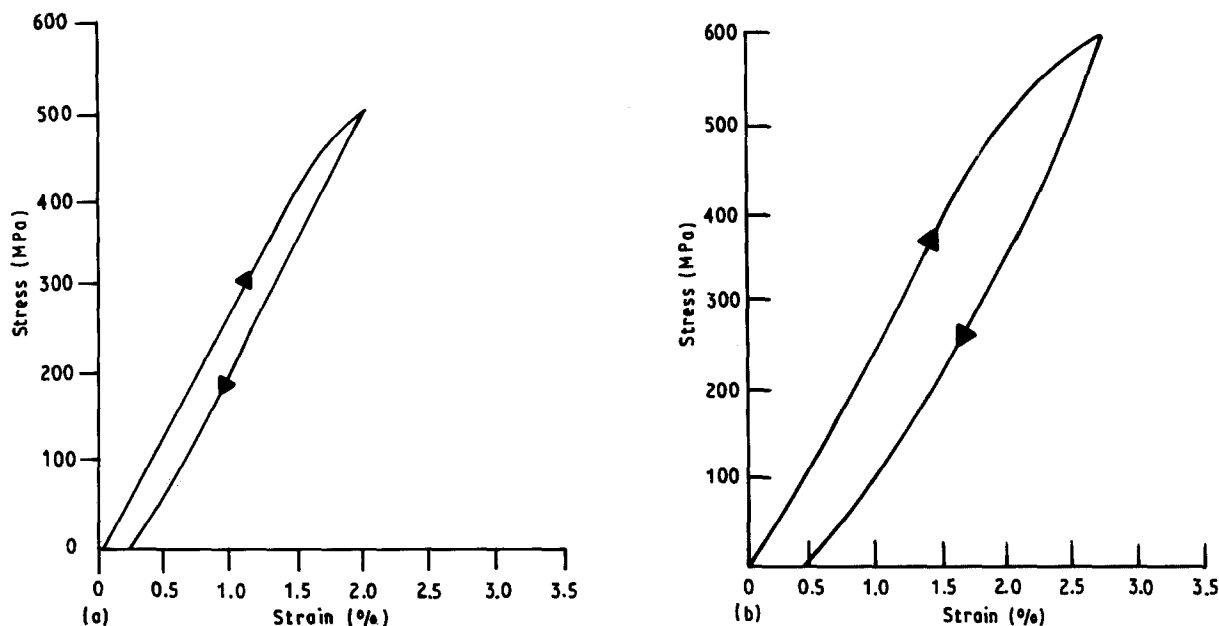


Figure 9 Stress-strain curves for two consecutive runs of a 3 mol %  $Y_2O_3$ - $ZrO_2$  ( $t'$ ) polycrystal stressed in uniaxial compression at 1000 °C (longitudinal direction). Note that the yield stress increased from run 1 to run 2.

taken to failure. The sample was unloaded once a stress of 500 MPa had been reached. It was cooled, X-rayed and loaded in run 2 at 1000 °C to a stress of about 600 MPa. In run 2 the sample behaved elastically up to 500 MPa, at which we had stopped loading on the first run. This behaviour is typical in many strain-hardened materials. It also indicates that domains that had switched between 450 and 500 MPa in the first run appear to have done so irreversibly, and did not switch again in run 2. In this second run 0.68% strain was produced through plastic deformation. Since the  $c/a$  ratio for this specimen was again about 1.013, a maximum of around 0.43% total plastic strain would be expected if ferroelastic domain switching were the only plastic deformation mechanism in operation. Dislocation motion may again be a possible mechanism contributing to the observed plasticity.

Dislocation movement has been shown to occur in yttria-doped TZP at elevated temperatures due to grain boundary sliding and creep cavitation within a thin ( $< 10 \mu m$ ) glassy phase present at the grain boundaries [26, 27]. This glassy phase is due to impurities such as  $SiO_2$  and  $Al_2O_3$  existing in the material [28]. XRD traces indicate that no monoclinic phase existed on any of the sample surfaces, as expected. Upon loading the Young's moduli were identical in each of the two runs. The difference in moduli observed during loading and unloading was smaller than that observed for the single crystal. These observations are consistent with the fact that in polycrystalline materials fewer grains are of a favourable orientation for switching to occur. Hence, any anisotropy caused by ferroelastic behaviour would be more subdued. This is evinced by the data shown in Table II,

TABLE II Average values of XRD data for 3 mol %  $Y_2O_3$ - $ZrO_2$  ( $t'$ ) polycrystal

	$I_{002}/I_{200}$ (peak height)	$I_{002}/I_{200}$ (integrated intensity)
Front lateral face at 25 °C		
Before stress	1.8	1.8
After stress, run 1	2.4	2.2
After stress, run 2	3.1	2.6
Rear lateral face at 25 °C		
Before stress	1.7	1.6
After stress, run 1	2.7	2.5
After stress, run 2	3.1	3.0
Right lateral face at 25 °C		
Before stress	0.9	1.0
After stress, run 2	1.5	1.5
Front lateral face at 1000 °C		
Before stress	1.3	1.7
After stress, run 1	2.1	1.9
After stress, run 2	3.4	2.2

which summarizes average values of XRD data, again indicating an increasing degree of reorientation of some of the variants in the sample with increasing stress, in agreement with the ferroelastic domain switching mechanism. Some average values for XRD data obtained at 1000 °C are also included in the table. Figs 10 and 11 demonstrate this switching phenomenon through some actual XRD traces, along with

their deconvoluted peaks. From these traces it is clear that some switching had occurred before loading due to the compressive stresses involved in surface grinding [14]. Here again,  $I_{002}$  increased at the expense of  $I_{200}$  in accordance with ferroelastic theory.

Partial hysteresis loops under compressive stress at room temperature have also been observed in this material, as seen in Fig. 12. XRD data again support

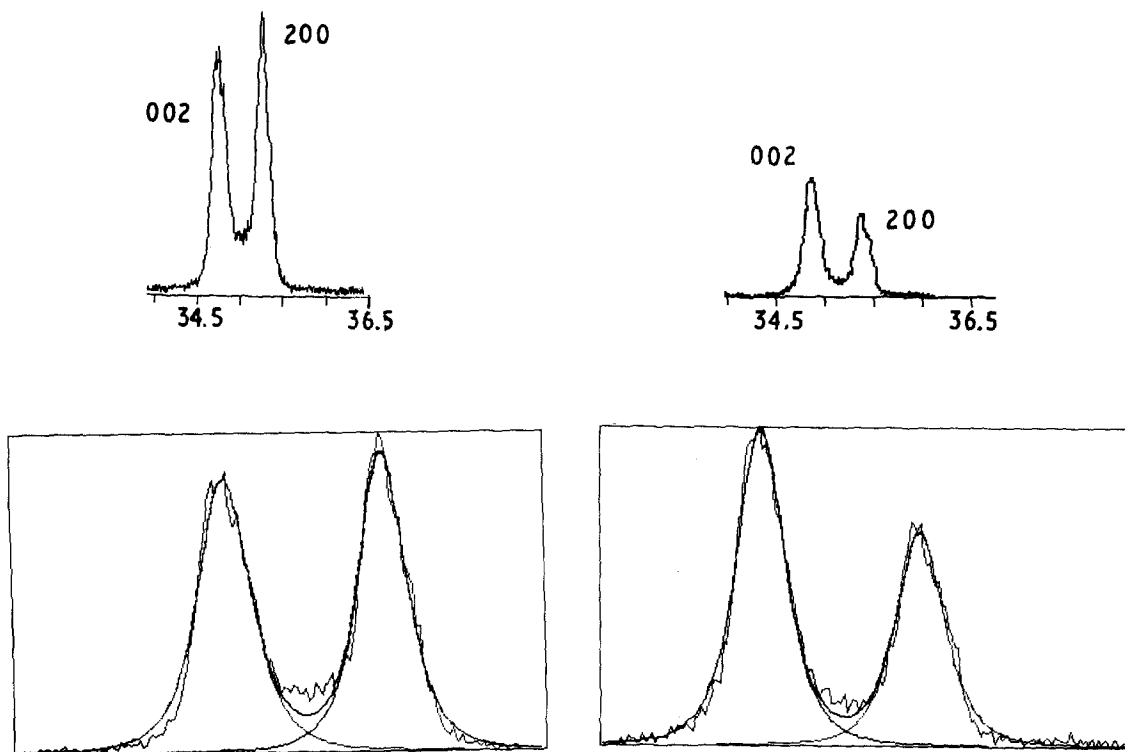


Figure 10 Room-temperature X-ray diffraction traces and deconvolutions (left) before and (right) after stress in 3 mol%  $Y_2O_3$ - $ZrO_2$  ( $t'$ -phase) polycrystal (right lateral face).

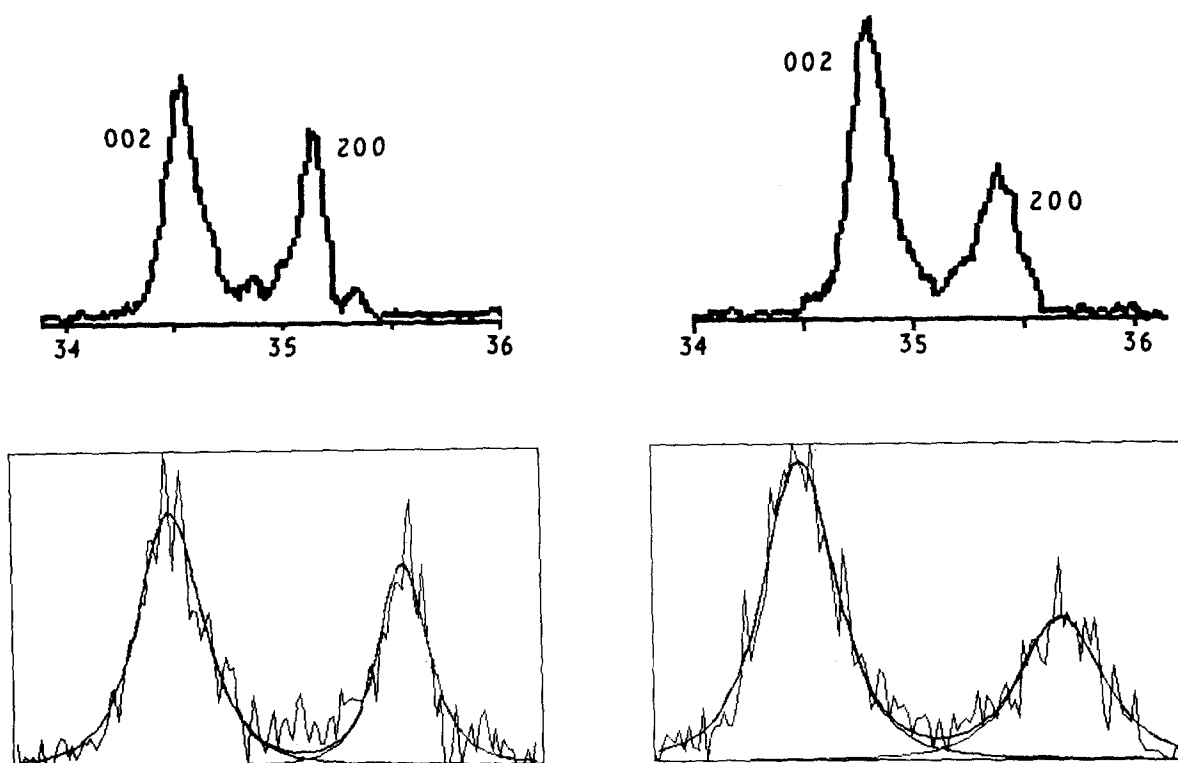


Figure 11 High-temperature (1000 °C) X-ray diffraction traces and deconvolutions (left) before and (right) after stress in 3 mol%  $Y_2O_3$ - $ZrO_2$  ( $t'$ -phase) polycrystal (front lateral face).

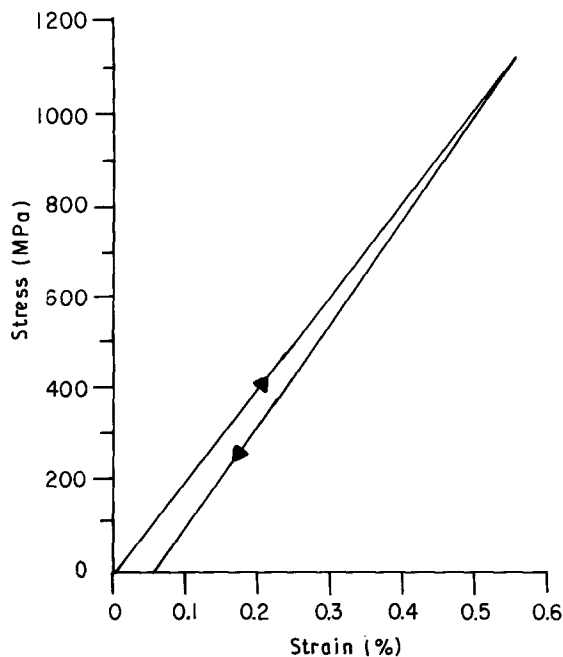


Figure 12 Partial hysteresis loop for a 3 mol %  $Y_2O_3$ - $ZrO_2$  ( $t'$ ) polycrystal stressed in uniaxial compression at room temperature.

the ferroelastic domain switching mechanism as being partially responsible for the plastic deformation.

#### 4. Summary and conclusions

From this study it is possible to draw a number of conclusions. The first is that ferroelastic domains are, indeed, present in 3 mol % yttria-doped zirconia existing in single-crystalline and polycrystalline forms ( $t'$ -phase).

Secondly, 3 mol % yttria-doped zirconia existing in single-crystalline and polycrystalline forms ( $t'$ -phase) undergoes ferroelastic domain switching when loaded in uniaxial compression at 1000°C. This contributes to the partial hysteresis loops observed in the stress-strain curves.

The third, and perhaps most significant, conclusion is that ferroelastic domain formation and/or switching is a deformation process and can expend mechanical energy that might otherwise be used for crack formation and propagation. It is therefore a potential toughening mechanism in ferroelastic materials. This also implies that care must be exercised when attributing deformation zone size to phase transformation alone when dealing with such theories as the "crack-shielding effect".

#### Acknowledgements

Jong Chen of the University of Utah is gratefully

acknowledged for his help with the TEM micrographs used in this paper. This research was supported by DARPA (through AFOSR Contract F49620-89-C-0054) and subcontracted through Ceramtec Inc., to the University of Utah.

#### References

1. K. AIZU, *J. Phys. Soc. Jpn.* **27** (1969) 387.
2. A. VIRKAR and R. MATSUMOTO, *J. Amer. Ceram. Soc.* **69** (1986) C224.
3. G. SRINIVASAN, J. JUE and A. VIRKAR, *ibid.* **72** (1989) 2098.
4. J. JUE and A. VIRKAR, *ibid.* **73** (1990) 3650.
5. J. JUE, J. CHEN and A. VIRKAR, *ibid.* **74** (1991) 1811.
6. A. HEUER, R. CHAIM and V. LANTERI, *Acta Metall.* **35** (1987) 661.
7. T. SAKUMA, *J. Mater. Sci.* **22** (1987) 4470.
8. R. MILLER, J. SMIALEK and R. GARLICK, in "Advances in ceramics", Vol. 3, edited by A. Heuer and L. Hobbs (American Ceramic Society, Columbus, Ohio, 1981) p. 241.
9. M. HAYAKAWA, N. KUNTANI and M. OKA, *Acta Metall.* **37** (1989) 2223.
10. M. HAYAKAWA and M. OKA, *ibid.* **37** (1989) 2229.
11. H. SCOTT, *J. Mater. Sci.* **10** (1975) 1527.
12. E. LEVIN, C. ROBBINS and H. McMURDIE, in "Phase diagrams for ceramists", edited by M. Reser (American Ceramic Society, Columbus, Ohio, 1964) p. 140.
13. M. JAYARATNA, M. YOSHIMURA and S. SOMIYA, *J. Amer. Ceram. Soc.* **67** (1984) C240.
14. V. STUBICAN and J. HELLMANN, in "Advances in ceramics", Vol. 3, edited by A. Heuer and L. Hobbs (American Ceramic Society, Columbus, Ohio, 1981) p. 25.
15. V. STUBICAN, R. HINK and S. RAY, *J. Amer. Ceram. Soc.* **61** (1978) 17.
16. V. WADHAVAN, *Phase Transitions* **3** (1982) 3.
17. D. MICHEL, L. MAZEROLLES and M. PEREZ Y JORBA, *J. Mater. Sci.* **18** (1983) 2618.
18. *Idem*, in "Advances in ceramics", Vol. 12, edited by N. Claussen, M. Rühle and A. Heuer (American Ceramic Society, Columbus, Ohio, 1984) p. 131.
19. K. PRETTYMAN, Ph.D. thesis, University of Utah (1991).
20. J. BUCKLEY and D. BRASKI, *J. Amer. Ceram. Soc.* **50** (1967) 220.
21. S. TSUNEKAWA and H. TAKEI, *J. Phys. Soc. Jpn.* **40** (1976) 1523.
22. H. TAKEI and S. TSUNEKAWA, *J. Cryst. Growth* **38** (1977) 55.
23. R. DAUSKARDT, D. VEIRS and R. RITCHIE, *J. Amer. Ceram. Soc.* **72** (1989) 1124.
24. D. CLARKE and F. ADAR, *ibid.* **65** (1982) 284.
25. D. MARSHALL, M. SHAW, R. DAUSKARDT, R. RITCHIE, M. READEY and A. HEUER, *ibid.* **73** (1990) 2659.
26. A. DOMINGUEZ-RODRIGUEZ, K. LAGERLOF and A. HEUER, *ibid.* **69** (1986) 281.
27. A. HEUER, V. LANTERI and A. DOMINGUEZ-RODRIGUEZ, *Acta Metall.* **37** (1989) 559.
28. J. LANKFORD and R. PAGE, *J. Mater. Sci.* **23** (1988) 4144.

Received 5 April

and accepted 30 July 1991